Motion-form interactions beyond the motion integration level: Evidence for interactions between orientation and optic flow signals

Andrea Pavan
Universität Regensburg, Institut für Psychologie, Regensburg, Germany

Rosilari Bellacosa Marotti
Department of General Psychology, University of Padua, Padua, Italy

George Mather
School of Psychology, University of Lincoln, Lincoln, United Kingdom

Motion and form encoding are closely coupled in the visual system. A number of physiological studies have shown that neurons in the striate and extrastriate cortex (e.g., V1 and MT) are selective for motion direction parallel to their preferred orientation, but some neurons also respond to motion orthogonal to their preferred spatial orientation. Recent psychophysical research (Mather, Pavan, Bellacosa, & Casco, 2012) has demonstrated that the strength of adaptation to two fields of transparently moving dots is modulated by simultaneously presented orientation signals, suggesting that the interaction occurs at the level of motion integrating receptive fields in the extrastriate cortex. In the present psychophysical study, we investigated whether motion-form interactions take place at a higher level of neural processing where optic flow components are extracted. In Experiment 1, we measured the duration of the motion aftereffect (MAE) generated by contracting or expanding dot fields in the presence of either radial (parallel) or concentric (orthogonal) counterphase pedestal gratings. To tap the stage at which optic flow is extracted, we measured the duration of the phantom MAE (Weisstein, Maguire, & Berbaum, 1977) in which we adapted and tested different parts of the visual field, with orientation signals presented either in the adapting (Experiment 2) or nonadapting (Experiments 3 and 4) sectors. Overall, the results showed that motion adaptation is suppressed most by orientation signals orthogonal to optic flow direction, suggesting that motion-form interactions also take place at the global motion level where optic flow is extracted.

Introduction

Form and motion information continuously interact. Cooperation between motion and form systems is necessary when each process alone is not sufficient, for example, when the visual system has to extract a partially occluded object or to judge its direction accurately. This view has recently been supported by neurophysiological and psychophysical studies that show how form (e.g., orientation) signals affect the extraction of motion and vice versa (Barlow & Olshausen, 2004; De Valois & De Valois, 1991; Edwards & Crane, 2007; Fu, Shen, Gao, & Dan, 2004; Geisler, 1999; Geisler, Albrecht, Crane, & Stern, 2001; McGraw, Walsh, & Barrett, 2004; McGraw, Whitaker, Skillen, & Chung, 2002; Pack & Born, 2001; Pack, Livingstone, Duffy, & Born, 2003; Pavan & Mather, 2008; Whitney, 2002). These interactions implement a continuous exchange of information between different processing stages and have been proposed to play a part in the distributed analysis of visual features (Beck & Neumann, 2010).

There is neurophysiological evidence for neurons that respond to both form and motion in several cortical sites, including early visual areas and extrastriate areas such as MT. Some V1 neurons, for example, respond to motion parallel to their preferred orientation rather than to motion orthogonal to the orientation of the receptive field (Geisler et al., 2001; Jancke, 2000); some MT neurons are also sensitive to motion parallel to their preferred orientation (Albright,

Citation: Pavan, A., Marotti, R. B., & Mather, G. (2013). Motion-form interactions beyond the motion integration level: Evidence for interactions between orientation and optic flow signals. *Journal of Vision*, *13*(6):16, 1–13, http://www.journalofvision.org/content/13/6/16, doi:10.1167/13.6.16.

doi: 10.1167/13.6.16 Received October 19, 2012; published May 31, 2013 ISSN 1534-7362

1984; Maunsell & Van Essen, 1983). Psychophysically, motion-form interactions have been shown to play a role in both direction and speed discrimination (Burr & Ross, 2002; Geisler, 1999; Krekelberg, Dannenberg, Hoffmann, Bremmer, & Ross, 2003; Ross, 2004).

Recent psychophysical research has used the motion aftereffect (MAE) to investigate the processing level at which form-motion interactions occur and provided evidence that interactions take place at the level of motion integration (Mather et al., 2012). The advantage of the MAE is that it can be used to tap into particular levels of processing in the motion system. For example, transparently moving bidirectional adapting fields normally produce a unidirectional MAE in the direction opposite to the vector combination (e.g., vector average) of the adapting directions, and this is thought to reflect changes in activity at the level of motion integration (Alais, Verstraten, & Burr, 2005; Mather, 1980; van der Smagt, Verstraten, & van de Grind, 1999; Verstraten, Fredericksen, & van de Grind, 1994; Verstraten, van der Smagt, Fredericksen, & van de Grind, 1999; von Grünau, 2002). Mather et al. (2012) used a bidirectional adapter containing transparently and orthogonally moving dots and found that the strength of motion adaptation was modulated by simultaneously presented orientation signals. If the orientation of a superimposed grating during adaptation was orthogonal to the resulting unidirectional MAE, the strength of the MAE was decreased relative to the condition in which the grating was parallel to the resulting MAE direction. These findings provide evidence that form and motion interact at the global motion level where moving components are integrated.

At the highest levels of motion processing in the visual system, associated with cortical area MST, neurons encode the global patterns of motion (optic flow) usually created by forward locomotion through the environment (Graziano, Andersen, & Snowden, 1994; Tanaka & Saito, 1989). At least 25% to 35% of neurons present in the dorsal part of the area MST (i.e., MSTd) in the macaque visual system have large receptive fields (from 10° up to 100°; Desimone & Ungerleider, 1986; Tanaka & Saito, 1989) and show selectivity to optic flow and to its components (Duffy & Wurtz, 1991b; Graziano et al., 1994; Lagae, Raiguel, & Orban, 1993; Saito et al., 1986; Sakata, Shibutani, Ito, & Tsurugai, 1986; Sakata, Shibutani, Kawano, & Harrington, 1985; Tanaka, Fukada, & Saito, 1989; Tanaka et al., 1986; Tanaka & Saito, 1989). Forward locomotion is also likely to generate global form information, namely, radial patterns of motion streaks caused by the temporal integration of responses to the expanding visual scene, and there is evidence for neurons in the form-processing stream, which are sensitive to these radial streak patterns (Gallant, Braun, & Van Essen, 1993; Ostwald, Lam, Li, & Kourtzi, 2008). The visual system may take advantage of the close correspondence between the visual form and motion information generated by locomotion, combining the two during high-level optic flow processing. The present study employed an adaptation paradigm to test for the presence of interactions between form and motion in optic flow processing. Experiment 1 used a similar paradigm to that reported in Mather et al. (2012), adapting to radial motion (i.e., contracting/expanding patterns) with superimposed stationary radial (parallel) or concentric (orthogonal) gratings. On the basis of the earlier results, we predict that MAEs obtained using radial (parallel) gratings will be stronger than those obtained using concentric gratings.

Experiment 1

Method

Participants

One author and nine naïve observers participated in the experiment. All participants had normal or corrected-to-normal visual acuity, participated voluntarily with no compensation, and gave their informed consent prior to their inclusion in the experiment.

Apparatus

Observers sat in a dark room at a distance of 57 cm from the screen. Viewing was binocular. Stimuli were displayed on a 19-inch CTX CRT Trinitron monitor with a refresh rate of 60 Hz and generated using Matlab Psychtoolbox (Brainard, 1997; Pelli, 1997). The screen resolution was 1280 × 1024 pixels. Each pixel subtended 1.8 arcmin. The mean luminance was 46.7 cd/m^2, measured using a Minolta LS-100 photometer. Stimuli were generated using a gamma-corrected lookup table to ensure display linearity.

Stimuli

Three different adapting stimuli were used: (a) a field of dots that moved coherently along radial trajectories, either contracting or expanding; (b) a field of radially moving dots with a superimposed counterphase flickering radial grating oriented parallel to the dots' trajectory; and (c) a field of radially moving dots with a superimposed counterphase flickering circular grating oriented orthogonal to the dots' trajectory. The dot field consisted of a dense spatial array of 1,444 coherently moving white dots (101 cd/m^2) displayed within a circular window with a diameter of 27° at the center of the screen (density: 2.5 dot/°^{2}). The luminance

of the background was set at 46.7 cd/m^2. The diameter of each dot was 0.12°, and all dots moved at 7.3°/s. The local speed of each dot did not vary with distance from the origin. Morrone, Tosetti, Montanaro, Fiorentini, Cioni, and Burr (2000) found no differences between the blood-oxygen-level-dependent (BOLD) responses to rigidly rotating patterns (where local speed varied with radius) and those with constant local speed.

To aid fixation at the focus of expansion, a gray disk (1° diameter) of the same mean luminance as the background was displayed and a white fixation point (0.2° diameter) positioned at the center of the gray disk. The fixation point overlapped with the center of the screen and thus the origin of the radial motion. Dots had a limited lifetime; that is, after 633.3 ms, each dot vanished and was replaced by a new dot at a different randomly selected position within the circular window. In addition, moving dots that traveled outside the window were also replaced by a new dot at a different randomly location within the circular window. The pedestal gratings had a diameter of 27° and overlapped with the circular window containing dots (Figure 1A). The radial and circular gratings were defined as follows:

$$Radial = m\cos(2\pi fu + \varphi) \quad (1)$$

where $u = arctgx(y/x)$, m is the contrast modulation of the cosine-wave, f is the angular frequency (i.e., 56/360), and φ is the phase shift of the cosine-wave.

$$Circular = m\cos\left(\frac{rs}{d2\pi + \varphi}\right) \quad (2)$$

where $r = (x^2 + y^2)^{(1/2)}$, $s = [(\sqrt{d^2 + d^2} - \sqrt{x^2 + y^2})/Nc]$, d is the diameter of the pattern (i.e., 27°), and Nc is the number of cycles (i.e., 18). In the case of the circular grating, the parameter s increases the spatial frequency of the grating as a function of the radius; this was implemented because in the case of radial gratings, the width of the bars shrinks with a decrease in the distance from the origin (Figure 1A), thus creating an increment of the spatial frequency. Gratings were counterphase flickered at 1 Hz to avoid the buildup of after images. The Michelson contrast of the gratings was set at 0.3.

Procedure

The procedure was the same as that reported in Mather et al. (2012). Observers were instructed to maintain fixation at the center of the screen. Each block started with an initial adaptation period of 60 s, followed immediately by the test stimulus, which lasted until the observer's response. Observers had to press the spacebar when any MAE ceased. Then, after a 1-s intertrial interval, top-up adaptation periods of 30 s alternated with test presentations and MAE measures (Figure 1B). The direction of adaptation and, if

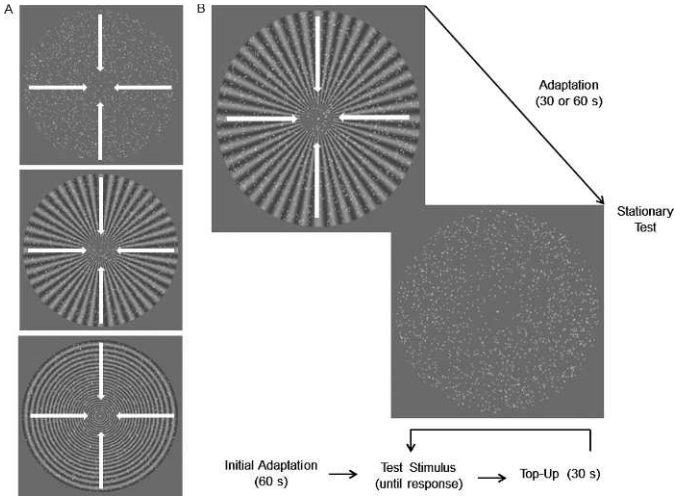

Figure 1. (A) Adapting patterns in Experiment 1: 1,444 white dots (diameter 0.12°) moving coherently either in expansion or contraction (only contracting motion is shown). The top panel shows the condition with no pedestal grating, the middle panel shows contracting moving dots on a radial pedestal grating (parallel to motion), and the bottom panel shows contracting moving dots on a circular pedestal (orthogonal to motion). (B) Schematic representation of the adapting procedure. Following 60 s of adaptation (the first trial) or 30 s of top-up adaptation, a stationary test pattern was presented. The adapting stimulus consisted of a field of 1,444 coherently contracting or expanding moving dots (only contracting motion is shown superimposed to a radial grating), whereas the test pattern was a field of 1,444 stationary dots and lasted until a participant's response.

present, the type of grating were kept constant within each block. The experiment involved six blocks: three pedestal conditions (i.e., no pedestal, parallel pedestal, and orthogonal pedestal) × two motion directions (i.e., contracting and expanding). Each block consisted of 10 trials.

Results

Figure 2 shows the mean MAE duration in each pedestal condition and for the two motion directions. A two-factor repeated-measures analysis of variance (ANOVA) was conducted, including Pedestal Condition (i.e., no pedestal, parallel pedestal, and orthogonal pedestal) and Motion Direction (contracting and expanding) as factors. There was a significant effect of Pedestal, $F(2, 18) = 13.76$, $p = 0.0001$, *partial*-$\eta^2 = 0.60$, and Motion Direction, $F(1, 9) = 15.25$, $p = 0.004$, *partial*-$\eta^2 = 0.63$, but no significant interaction between Motion Direction and Pedestal, $F(2, 18) = 0.39$, $p = 0.68$, *partial*-$\eta^2 = 0.042$. Because we found a significant effect of Motion Direction but no interaction between Motion Direction and Pedestal, we performed separate

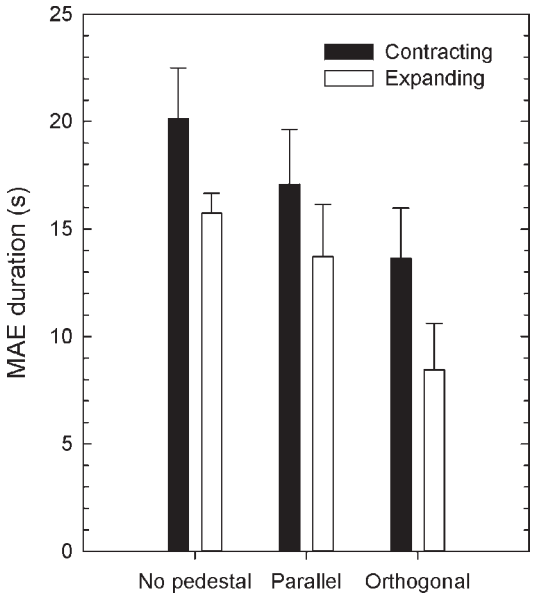

Figure 2. Mean MAE duration (s) after adaptation to a field of radially moving dots (contracting or expanding) with no pedestal, and with superimposed radial (parallel) or circular (orthogonal) pedestal gratings. Error bars ± *SEM*.

repeated-measures ANOVAs to assess the effect of the pedestal separately for each motion type.

For contracting motion, a repeated-measures ANOVA showed an effect of Pedestal, $F(2, 18) = 6.13$, $p = 0.009$, *partial*-$\eta^2 = 0.41$. Simple contrasts found a significant difference between the orthogonal and the no-pedestal conditions, $F(1, 9) = 13.85$, $p = 0.005$, *partial*-$\eta^2 = 0.61$, but no significant difference between the parallel and the no-pedestal conditions, $F(1, 9) = 2.54$, $p = 0.14$, *partial*-$\eta^2 = 0.22$. Similarly, for expanding motion, a repeated-measures ANOVA found a significant effect of Pedestal, $F(2, 18) = 12.63$, $p = 0.0001$, *partial*-$\eta^2 = 0.58$. Simple contrasts revealed a significant difference between the orthogonal pedestal and the no-pedestal conditions, $F(1, 9) = 51.39$, $p = 0.0001$, *partial*-$\eta^2 = 0.85$, but no significant difference between the parallel pedestal and the no-pedestal conditions, $F(1, 9) = 2.38$, $p = 0.16$, *partial*-$\eta^2 = 0.21$.

Discussion

The results of Experiment 1 show that the addition of a pedestal grating orthogonal to radially moving dots significantly reduced the duration of the MAE relative to the no-pedestal condition, this for both contracting and expanding patterns. On the other hand, when a radial (parallel) pedestal was added, we found no significant reduction of the MAE duration relative to the no-pedestal control condition. The longer MAE duration obtained with parallel (radial) pedestals relative to the orthogonal condition is consistent with a motion-form interaction, which favors motion trajectories parallel to local orientation signals (Mather et al., 2012). In addition, we found an asymmetry between contracting and expanding motion, with adaptation to contracting motion producing longer MAE duration. This latter result is consistent with previous findings (Bakan & Mizusawa, 1963; Reinhardt-Rutland, 1994; Scott, Lavender, McWhirt, & Powell, 1966).

The results of Experiment 1 do not necessarily reflect form-motion interactions at the level of optic flow processing, even though the experiment employed radial motion. Large receptive fields sensitive to optic flow can be constructed by combining the outputs of many smaller motion-selective receptive fields, whose preferred directions and retinal locations are arranged to form a radial pattern. The results of Experiment 1 could reflect form-motion interactions that take place at the level of these smaller receptive fields (as measured by Mather et al., 2012), which are then inherited by neurons tuned to optic flow. To investigate the level at which the form-motion interaction occurs, we exploited the well-known phantom MAE (Snowden & Milne, 1997; Weisstein et al., 1977), in which adaptation to some parts/sectors of the visual field that contain expanding or contracting motion subsequently induces the perception of contracting or expanding motion in other (nonadapted) parts of the visual field. The phantom MAE is thought to depend on detectors with large receptive fields that are sensitive to various components of object or self-movement (Burr, Morrone, & Vaina, 1998; Desimone & Ungerleider, 1986; Duffy & Wurtz, 1991a; Graziano et al., 1994; Lagae, Maes, Raiguel, Xiao, & Orban, 1994; Morrone, Burr, & Vaina, 1995; Regan & Beverly, 1985; Snowden & Milne, 1996, 1997; Tanaka & Saito, 1989). In Experiment 2, the adapting pattern (with superimposed radial or circular pedestal grating) was presented in only some stimulus sectors, and the test pattern was presented in the nonadapted sectors of the visual field.

Experiment 2

Method

Participants

Two authors and a new sample of eight naïve observers participated. All participants had normal or corrected-to-normal visual acuity, participated voluntarily with no compensation, and gave their

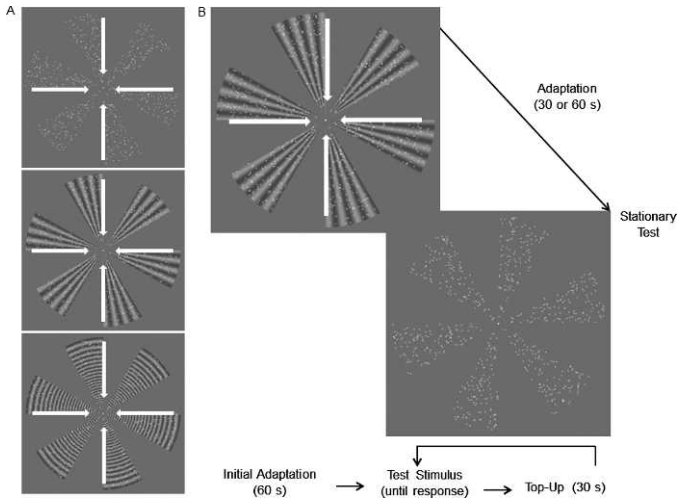

Figure 3. (A) Adapting patterns in Experiment 2: 720 dots moving coherently either in expansion or contraction in six circular sectors (only contracting motion is shown). The top panel shows the condition with no pedestal grating (dots are displayed in six sectors of 30° each), the middle panel shows contracting moving dots on radial pedestal gratings, and the bottom panel shows contracting moving dots on circular pedestals. (B) Schematic representation of the adapting procedure. The test pattern was a field of 720 stationary dots displayed in the nonadapted sectors.

informed consent prior to their inclusion in the experiment.

Apparatus

The apparatus was the same used in Experiment 1.

Stimuli and procedure

Stimuli were similar to those used in Experiment 1, with the exception that subjects were adapted to radially moving dots present in six circular sectors (Figure 3A). Each sector subtended an angle of 30°. Similarly to Experiment 1, three different stimulus conditions were employed: (a) dots moving coherently along radial trajectories, either contracting or expanding, presented in alternating circular sectors (no pedestal condition); (b) radially moving dots presented in six alternating circular sectors superimposed on a counterphase flickering radial grating (parallel pedestal condition); and (c) radially moving dots in six alternating circular sectors, superimposed on a counterphase flickering circular grating (orthogonal pedestal condition). To maintain the same dot density as in the Experiment 1, we used 120 dots per sector (2.5 dot/$^{\circ 2}$). All the other parameters were the same as in Experiment 1.

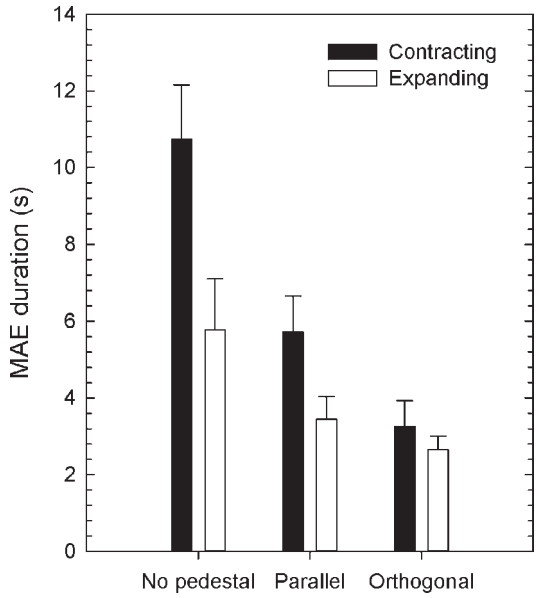

Figure 4. Mean phantom MAE duration (s) after adaptation to a field of radially moving dots (contracting or expanding) with no pedestal and with superimposed radial (parallel) or circular (orthogonal) pedestals. Error bars ± *SEM*.

The procedure was the same as in Experiment 1, with the exception that during the test phase, stationary dots were displayed in the nonadapted sectors (Figure 3B). The direction of adaptation, adapting sectors, and, if present, the type of grating were kept constant within each block. The experiment involved six blocks: three pedestal conditions (i.e., no pedestal, parallel pedestal, and orthogonal pedestal) × two motion directions (i.e., contracting and expanding). Each block consisted of 10 trials.

Results

Figure 4 shows the results of Experiment 2. A two-factor repeated-measures ANOVA including Pedestal Condition and Motion Direction as factors found significant main effects of Pedestal, $F(2, 18) = 22.55$, $p = 0.0001$, *partial*-$\eta^2 = 0.72$, and Motion Direction, $F(1, 9) = 10.31$, $p = 0.011$, *partial*-$\eta^2 = 0.53$, and a significant interaction between Motion Direction and Pedestal, $F(2, 18) = 4.04$, $p = 0.036$, *partial*-$\eta^2 = 0.31$. Bonferroni-corrected pairwise comparisons showed a significant difference between contracting and expanding patterns for the no-pedestal and the parallel pedestal conditions ($p = 0.021$ and $p = 0.034$, respectively). For the Pedestal factor, planned simple contrasts found a significant difference between the orthogonal and the no-pedestal conditions, $F(1, 9) = 28.14$, $p = 0.0001$, *partial*-$\eta^2 = 0.76$, and a significant difference between the parallel and the no-pedestal conditions, $F(1, 9) = 19.19$, $p = 0.002$, *partial*-$\eta^2 = 0.68$.

Discussion

The overall duration of the phantom MAE is shorter than the duration of the concrete MAE in Experiment 1. Moreover, the addition of oriented pedestals reduces the phantom MAE duration relative to the control condition, with a greater reduction when using circular (orthogonal) pedestals than radial (parallel) pedestals. Results also showed a pronounced asymmetry between the duration of phantom MAEs produced with contracting and expanding patterns, with a much longer duration when adapting to contracting motion, at least for the no-pedestal and parallel pedestal conditions (Figure 4).

The adaptation measured by the phantom MAE in Experiment 2 is likely to take place at the level of global optic flow processing (probably MST), where detectors have large receptive fields that encompass wide portions of the visual fields, respond to large moving stimuli, are position invariant (Duffy & Wurtz, 1991a, 1991b; Graziano et al., 1994; Orban et al., 1992; Saito et al., 1986; Tanaka & Saito, 1989), and respond to stimuli with parts removed (Tanaka et al., 1989). However, although Experiment 2 succeeded in isolating high-level adaptation, it is still possible that the motion-form interaction that produces different levels of adaptation is already present in the responses that arrive at the optic flow processing stage, because in Experiment 2, dots and grating were superimposed. Experiment 3 attempted to isolate a form-motion interaction at the optic flow level itself, by presenting the moving dots and pedestal gratings in different sectors during the adaptation period. The rationale was that if pedestals are still effective in suppressing the phantom MAE, then the underlying motion-form interaction cannot be mediated by small, low-level receptive fields but must involve large fields that encompass nonoverlapping stimulus elements.

Experiment 3

Method

Participants

Two authors and a new sample of eight naïve observers participated. All participants had normal or corrected-to-normal visual acuity, participated voluntarily with no compensation, and gave their informed consent prior to their inclusion in the experiment.

Apparatus

The apparatus was the same used in the previous experiments.

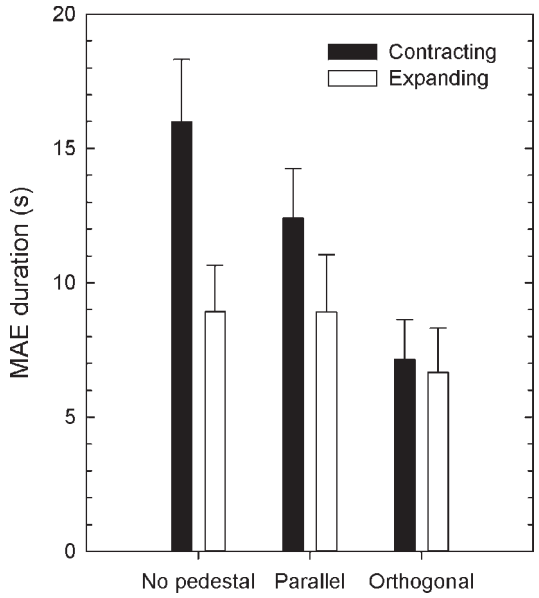

Figure 5. Mean phantom MAE duration (s) after adaptation to six fields (central angle of 30°) of radially moving dots (contracting or expanding) with no pedestal and with pedestals either radial (parallel) or circular (orthogonal) presented in the nonadapting sectors during the adapting period. Error bars ± *SEM*.

Stimuli and procedure

Stimuli were similar to those used in Experiment 2, with the exception that during the adapting phase, radially moving dots and pedestal gratings were presented in adjacent sectors. All of the other parameters were the same as in the previous experiments. The procedure was the same as in the previous experiment, with stationary test dots displayed in the sectors that previously contained no adapting motion. The direction of adaptation, adapting sectors, and, if present, the type of grating were kept constant within each block. The experiment involved six blocks: three pedestal conditions (i.e., no pedestal, parallel pedestal, and orthogonal pedestal) × two motion directions (i.e., contracting and expanding). Each block consisted of 10 trials.

Results

Figure 5 shows the results of Experiment 3. A two-factor repeated-measures ANOVA including Pedestal Condition and Motion Direction as factors reported significant main effects of Pedestal, $F(2, 18) = 18.07$, $p = 0.0001$, *partial*-$\eta^2 = 0.67$, and Motion Direction, $F(1, 9) = 15.94$, $p = 0.003$, *partial*-$\eta^2 = 0.53$, and a significant interaction between Motion Direction and Pedestal, $F(2, 18) = 13.97$, $p = 0.0001$, *partial*-$\eta^2 = 0.61$.

Bonferroni-corrected pairwise comparisons indicated a significant difference between the two types of

motion for the no-pedestal and the parallel pedestal conditions ($p = 0.001$ and $p = 0.021$, respectively). For the Pedestal factor, planned simple contrasts reported a significant difference between the orthogonal and the no-pedestal conditions, $F(1, 9) = 29.27$, $p = 0.0001$, *partial*-$\eta^2 = 0.77$, but no a significant difference between the parallel and the no-pedestal conditions, $F(1, 9) = 4.74$, $p = 0.057$, *partial*-$\eta^2 = 0.35$.

Discussion

Experiment 3 found an effect of static pedestal orientation on the strength of motion adaptation even when it was not presented in the same sectors as the moving adapting pattern. Inspection of the data reveals three interesting points: (a) the duration of the phantom MAE is on average longer relative to the durations measured in Experiment 2, suggesting a weaker adaptation suppression when moving dots and pedestal gratings are displayed in separate sectors; (b) the asymmetry between the two motion directions is present at the global level; and (c) circular orthogonal pedestals produce higher suppression of the phantom MAE relative to the parallel pedestal. Results are likely to reflect interactions at the global level at which optic flow is extracted (i.e., MST); however, because of the narrow size of the sectors (30°) and the size of some MT-receptive fields (up to 25°; Felleman & Kaas, 1984), these effects could still rely on some local interactions between motion and orientation. This is because MT-receptive fields could straddle the boundaries between motion and grating sectors. To rule out this possibility, we performed an additional experiment using a stimulus configuration similar to that employed by Snowden and Milne (1997), in which the central angle of each sector was 90°. In this case, sectors are much wider than the maximum size of the receptive fields of MT neurons, and the axis of the mean directions of the phantom MAE would be nearly orthogonal to the axis of the mean directions of adaptation (Snowden & Milne, 1997).

Experiment 4

Method

Participants

Two authors and a new sample of eight naïve observers participated. All participants had normal or corrected-to-normal visual acuity, participated voluntarily with compensation, and gave their informed consent prior to their inclusion in the experiment.

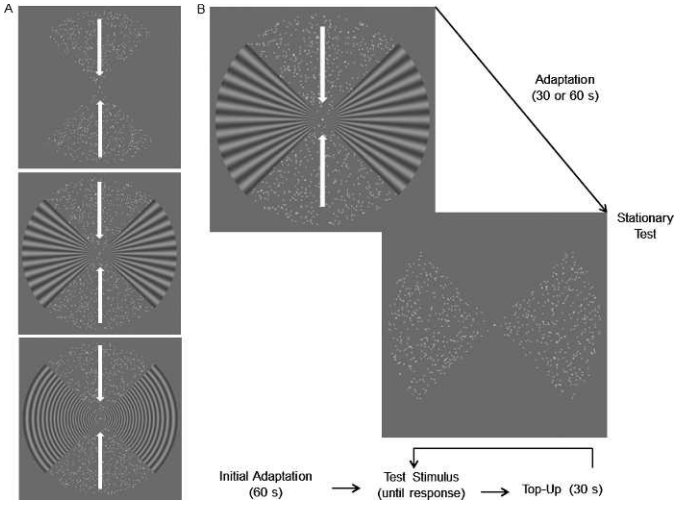

Figure 6. (A) Adapting patterns in Experiment 4: 720 dots moving coherently either in expansion or contraction in two circular sectors (only contracting motion is shown). The top panel shows the condition with no pedestal grating (dots are displayed in two sectors of 90° each), the middle panel shows contracting moving dots with radial pedestal gratings displayed in the nonadapting sectors, and the bottom panel shows contracting moving dots with circular pedestals gratings displayed in the nonadapting sectors. (B) Schematic representation of the adapting procedure. The test pattern was a field of 720 stationary dots displayed in the nonadapted sectors.

Apparatus

The apparatus was the same as used in previous experiments.

Stimuli and procedure

Stimuli were similar to those used in Experiment 3, with the exception that participants were adapted to radially moving dots presented in two circular sectors, with each sector subtending a central angle of 90° (Figure 6A). To maintain the same dot density as in the previous experiments, we used 360 dots per sector (2.5 dot/$^{\circ 2}$). Stimulus parameters, trial sequence, and procedure were the same as in Experiment 3 (Figure 6B).

Results

Figure 7 shows the results of Experiment 4. A two-factor repeated-measures ANOVA including Pedestal Condition and Motion Direction as factors reported significant main effects of Pedestal, $F(2, 18) = 6.14$, $p = 0.009$, *partial*-$\eta^2 = 0.41$, and Motion Direction, $F(1, 9) = 12.34$, $p = 0.007$, *partial*-$\eta^2 = 0.58$, but no significant interaction between Motion Direction and Pedestal, $F(2, 18) = 2.55$, $p = 0.11$, *partial*-$\eta^2 = 0.22$. Because we

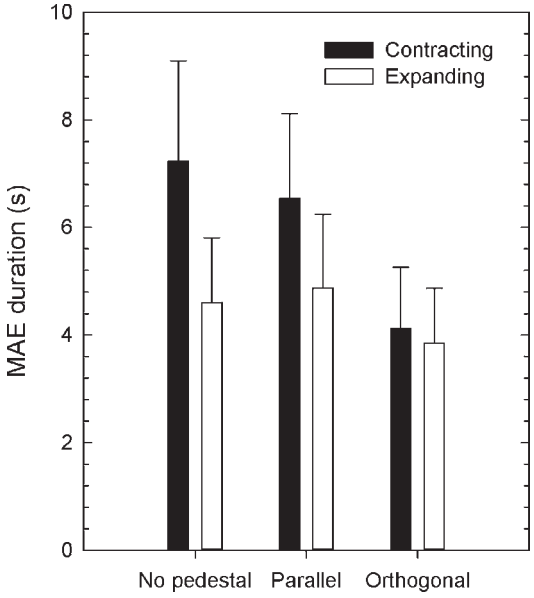

Figure 7. Mean phantom MAE duration (s) after adaptation to four sectors (central angle of 90°) of radially moving dots (contracting or expanding) with no pedestal and with pedestals either radial (parallel) or circular (orthogonal) presented in the nonadapting sectors during the adapting period. Error bars ± *SEM*.

found a significant effect of Motion Direction but no interaction between Motion Direction and Pedestal, we performed separate repeated-measures ANOVAs to assess the effect of the pedestal separately for each motion type.

For contracting motion, a repeated-measures ANOVA showed an effect of Pedestal, $F(2, 18) = 4.69$, $p = 0.023$, *partial*-$\eta^2 = 0.34$. Simple contrasts found a significant difference between the orthogonal and the no-pedestal conditions, $F(1, 9) = 6.08$, $p = 0.036$, *partial*-$\eta^2 = 0.40$, but no significant difference between the parallel and the no-pedestal conditions, $F(1, 9) = 0.36$, $p = 0.57$, *partial*-$\eta^2 = 0.04$. Similarly, for expanding motion, a repeated-measures ANOVA found a significant effect of Pedestal, $F(2, 18) = 3.94$, $p = 0.038$, *partial*-$\eta^2 = 0.30$. Simple contrasts revealed a significant difference between the orthogonal pedestal and the no-pedestal conditions, $F(1, 9) = 5.33$, $p = 0.046$, *partial*-$\eta^2 = 0.37$, but no significant difference between the parallel pedestal and the no-pedestal conditions, $F(1, 9) = 0.99$, $p = 0.35$, *partial*-$\eta^2 = 0.1$.

Discussion

The results of Experiment 4 confirm and generalize those of Experiment 3. The circular orthogonal pedestal produces higher suppression relative to the parallel pedestal, further suggesting that orientation-selective motion-form interactions are ubiquitous, being present at several levels of the motion processing hierarchy (Beck & Neumann, 2010; Mishkin, Ungerleider, & Macko, 1983) and favor orientation signals parallel to the motion trajectory (Mather et al., 2012). The results also confirm the presence of the asymmetry between the two motion directions and suggest that it maintains up to the level in which optic flow is processed. In addition, we found that the duration of the phantom MAE is, on average, shorter relative to the durations measured in Experiments 3 and 2. Price, Greenwood, and Ibbotson (2004) found that an increase in the arc subtended by the adapting sector reduced the strength of phantom MAE. They suggested that an increase in stimulus size would reduce the response of direction-selective neurons with inhibitory surrounds (Allman, Miezin, & McGuinness, 1985a, 1985b), thus reducing MAE strength. Similar conclusions were also drawn by Tadin, Lappin, Gilroy, and Blake (2003); although their stimuli selectively tapped the receptive fields of MT neurons, a surround suppression effect is likely to occur also at MST level. Indeed, there is physiological evidence that the monkey area MSTl largely responds to small moving patterns and decreases its response as the stimulus size increases (Tanaka, Sugita, Moriya, & Saito, 1993). Other authors report a similar subregion in the human MT+ complex (Bartel, Zeki, & Logothetis, 2008; Dukelow et al., 2001; Holliday & Meese, 2008).

General discussion

A series of four experiments found evidence for motion-form interactions at the level at which optic flow is extracted. Overall, orthogonal pedestal gratings are more effective in suppressing the duration of contracting/expanding adaptation compared with pedestals oriented parallel to the global pattern of motion. These results extend those presented in a previous article (Mather et al., 2012), in which we found evidence for motion-form interactions at the stage at which local motion signals are integrated to compute rigid pattern motion (e.g., MT).

The response properties of neurons in MST make them a likely neural substrate for the computation of optic flow, as mentioned earlier (e.g., Graziano et al., 1994; Tanaka & Saito, 1989). Furthermore, there is evidence for neurons tuned to the spatial patterns that would be created by the temporal smearing (motion streaks) of optic flow in area V4 (Gallant et al., 1993; Ostwald et al., 2008). The adaptation experiments reported here indicate that these two neural signals about forward locomotion and direction of heading interact. Niehorster, Cheng, and Li (2010) recently reported other evidence for such interactions. Partici-

pants made judgments of their apparent direction of heading, based on stimuli that contained a combination of motion (optic flow) and form (radial glass pattern). Results indicated that human heading perception is based on a combination of motion and form cues. Our results indicate that form-based responses selectively modulate motion responses (gain control), as indicated by adaptation strength.

There is neurophysiological and computational evidence that the complex tuning/selectivity to optic flow components showed by MST neurons derives from the integration of nonlinearly transformed local motion signals from MT (Mineault, Khawaja, Butts, & Pack, 2012; Paninski, 2004; Wu, David, & Gallant, 2006). Mineault et al. (2012) showed that the nonlinear integration (i.e., compressive nonlinearity; Martin & Hudspeth, 2001) introduced in their hierarchical model is necessary to increase the overall level of responses to optic flow components (e.g., spiral and deformation stimuli) relative to translational stimuli, while preserving the shape of the neurons' tuning curves. The interactions between complex moving patterns and polar pedestals we found in Experiment 1 could reflect local processes at the first stage of optic flow computation (i.e., MT) that integrate local motion information and local orientation signals (Albright, 1984; Hedges et al., 2011; Mather et al., 2012).

To selectively tap the level at which optic flow components are extracted, we exploited the phantom MAE (Snowden & Milne, 1997; Weisstein et al., 1977). In Experiment 2, using superimposed adapting sectors and polar gratings, we found a modulation of the adapting strength in the presence of polar gratings, but the circular grating (i.e., orthogonal pedestal) was much more effective in causing adaptation suppression. Although the phantom MAE is thought to selectively tap the activity of MST neurons (Snowden & Milne, 1996, 1997), the effect of the orientation/form information could still be inherited from lower levels when moving dots and polar pedestals are superimposed. Gallant et al. (1993) found evidence in area V4 for selectivity to stationary complex polar sinusoidal gratings. Because area V4 (V4d, the topographic homologue in humans; Tootell & Hadjikhani, 2001) is connected with area MT (Maunsell & Van Essen, 1983; Ungerleider & Desimone, 1986), it is possible that the motion-form interaction found in Experiment 2 derives from MT units that integrate local motion signals and orientation/form signals forwarded by V4(d). However, the results of Experiments 3 and 4 suggest that motion-form integration is likely to occur at the final stage of optic flow processing (i.e., MST) because adaptation sectors and polar gratings were not superimposed, thus requiring large receptive fields that encompass non-overlapping stimulus elements.

As reported in Mather et al. (2012), parallel pedestals produce longer adaptation than orthogonal pedestals. In three of the experiments reported here, there was no significant difference between MAE durations without a pedestal and durations with a parallel pedestal, although there was a hint of a reduction in duration with a parallel pedestal. In the remaining experiment (i.e., Experiment 2), there was a significant reduction in MAE duration using a parallel pedestal (also reported by Mather et al., 2012). But on the basis of the motion-streak model, one might expect an increase in the duration of MAEs in the presence of parallel pedestals. Two factors may work against finding such a facilitatory effect with our experimental stimuli, which relate to the fact that the "streaks" in the stimuli are actually dense, high-contrast grating bars. First, the pedestal grating may generate a high level of divisive normalization, which, from a computational perspective, is the ratio between the response of an individual neuron and the summed activity of a pool of neurons and is presumed to arise from lateral interconnections within a region (Britten & Heuer, 1999). There is evidence for normalization in both area V1 and MT (Heeger, 1992; Heeger, Simoncelli, & Movshon, 1996; Rust, Mante, Simoncelli, & Movshon, 2006; Simoncelli & Heeger, 1998). Second, the high-contrast pedestal grating may activate inhibitory motion deblurring mechanisms (Purushothaman, Ögmen, Chen, & Bedell, 1998), which are not selective for orientation and therefore affect both parallel and orthogonal motion. Thus, in the presence of pedestals, the resultant MAE may be affected by both orientation-selective enhancement from a streak mechanism and nonselective suppression from a gain-control or deblurring mechanism. Further empirical and computational work is needed to clarify the possible contributions of gain-control and deblurring mechanisms.

In the present study, we found an asymmetry between contracting and expanding motion. There is wide evidence for longer MAE durations following adaptation to contracting patterns (expanding aftereffect) compared with expanding patterns (contracting aftereffect; Bakan & Mizusawa, 1963; Reinhardt-Rutland, 1994; Scott et al., 1966), but the origin of such an asymmetry and its functional role remains to be determined. However, there is evidence that it can be reduced with practice (Scott et al., 1966). Bex, Metha and Makous (1998), for example, found that contrast detection thresholds for translational, radial, and rotating moving patterns were not significantly different and that suprathreshold contrast matches among the patterns were equal. Studies on motion sensitivity and reaction times have found that the perception of visual expansion is generally better than for contraction. Edwards and Badcock (1993) reported that

sensitivity was lower for contracting dot fields than for expanding dot fields, and Ball and Sekuler (1980) found that expanding motion evoked faster reaction times. Reinhardt-Rutland (1994) proposed that this asymmetry reflects probably habitual forward motion in human beings that may originate asymmetries in the structural nature of visual cortical areas involved in the processing of optic flow. The presence of an overrepresentation of expansion-selective cells found in MST (Graziano et al., 1994) may establish the ground of the Reinhardt-Rutland speculation.

In conclusion, motion-form interactions that favor parallel motion at the stage in which optic flow is extracted may be important for heading, object representation, and three-dimensional (3D) velocity estimation. Gallant et al. (1993) argued that cells selective for non-Cartesian stimuli might mediate the construction of the 3D structure of objects by acting as filters for the extraction of the relevant information from the retinal image. Such information would be subsequently used to build up a representation of the surface structure of objects from the observer's point of view (Horn & Brooks, 1989). The fact that MST is involved in fine estimation of motion direction and in the control of eye movements for maintaining fixation on moving 3D objects (Takemura, Murata, Kawano, & Miles, 2007) suggests that it exploits the 3D representation of the objects and that orientation information parallel to motion direction could facilitate the extraction of both direction (Burr & Ross, 2002) and 3D velocity, in addition to the nonlinear integration that is necessary for accurate calculation of the 3D velocity of motion in depth (Mineault et al., 2012).

Keywords: optic flow components, motion aftereffect, motion-form interaction, motion streak, divisive normalization

Acknowledgments

This work was supported by the Alexander von Humboldt Foundation, the University of Regensburg, the University of Lincoln, and the University of Padua. R.B.M. was supported by the CARIPARO foundation, and G.M. was supported by the Wellcome Trust (WT082816MA). We thank Martin Gall for data collection of Experiment 4.

Commercial relationships: none.
Corresponding author: Andrea Pavan.
Email: andrea.pavan@psychologie.uni-regensburg.de.
Address: Universität Regensburg, Institut für Psychologie, Regensburg, Germany.

References

Alais, D., Verstraten, F. A., & Burr, D. C. (2005). The motion aftereffect of transparent motion: Two temporal channels account for perceived direction. *Vision Research, 45,* 403–412.

Albright, T. D. (1984). Direction and orientation selectivity of neurons in visual area MT of the macaque. *Journal of Neurophysiology, 52,* 1106–1130.

Allman, J., Miezin, F., & McGuinness, E. (1985a). Direction-and velocity-specific responses from beyond the classical receptive field in the middle temporal visual area (MT). *Perception, 14,* 105–126.

Allman, J., Miezin, F., & McGuinness, E. (1985b). Stimulus specific responses from beyond the classical receptive field: Neurophysiological mechanisms for local-global comparisons in visual neurons. *Annual Review of Neuroscience, 8,* 407–430.

Bakan, P., & Mizusawa, W. A. K. (1963). Effect of inspection time and direction of rotation on a generalized form of the spiral after-effect. *Journal of Experimental Psychology, 65,* 583–586.

Ball, K., & Sekuler, R. (1980). Human vision favors centrifugal motion. *Perception, 9,* 317–325.

Barlow, H. B., & Olshausen, B. A. (2004). Convergent evidence for the visual analysis of optic flow through anisotropic attenuation of high spatial frequencies. *Journal of Vision*, *4*(6):1, 415–426, http://www.journalofvision.org/content/4/6/1, doi: 10.1167/4.6.1. [PubMed] [Article]

Bartel, A., Zeki, S., & Logothetis, N. K. (2008). Natural vision reveals regional specialization to local motion and to contrast-invariant, global flow in the human brain. *Cerebral Cortex, 18,* 705–717.

Beck, C., & Neumann, H. (2010). Interactions of motion and form in visual cortex: A neural model. *Journal of Physiology, 104,* 61–70.

Bex, P. J., Metha, A. B., & Makous, W. (1998). Psychophysical evidence for a functional hierarchy of motion processing mechanisms. *Journal of the Optical Society of America A, 15,* 769–776.

Brainard, D. H. (1997). The psychophysics toolbox. *Spatial Vision, 10,* 443–446.

Britten, K. H., & Heuer, H. W. (1999). Spatial summation in the receptive fields of MT neurons. *Journal of Neuroscience, 19,* 5074–5084.

Burr, D. C., Morrone, M. C., & Vaina, L. M. (1998). Large receptive fields for optic flow detection in humans. *Vision Research, 38,* 1731–1743.

Burr, D. C., & Ross, J. (2002). Direct evidence that speedlines influence motion mechanisms. *Journal of Neuroscience, 22,* 8661–8664.

De Valois, R. L., & De Valois, K. K. (1991). Vernier acuity with stationary moving Gabors. *Vision Research, 31,* 1619–1626.

Desimone, R., & Ungerleider, L. G. (1986). Multiple visual areas in the caudal superior temporal sulcus of the macaque. *Journal of Comparative Neurology, 248,* 164–189.

Duffy, C. J., & Wurtz, R. H. (1991a). Sensitivity of MST neurons to optic flow stimuli. I. A continuum of response selectivity to large-field stimuli. *Journal of Neurophysiology, 65,* 1329 –1345.

Duffy, C. J., & Wurtz, R. H. (1991b). Sensitivity of MST neurons to optic flow stimuli. II. Mechanisms of response selectivity revealed by small-field stimuli. *Journal of Neurophysiology, 65,* 1346 –1359.

Dukelow, S. P., DeSouza, J. F., Culham, J. C., van Den Berg, A. V., Menon, R. S., & Vilis, T. (2001). Distinguishing subregions of the human mt+ complex using visual fields and pursuit eye movements. *Journal of Neurophysiology, 86,* 1991–2000.

Edwards, M., & Badcock, D. R. (1993). Asymmetries in the sensitivity to motion in depth: A centripetal bias. *Perception, 22,* 1013–1023.

Edwards, M., & Crane, M. F. (2007). Motion streaks improve motion detection. *Vision Research, 47,* 828–833.

Felleman, D. J., & Kaas, J. H. (1984). Receptive-field properties of neurons in middle temporal visual area (MT) of owl monkeys. *Journal of Neurophysiology, 52,* 488–513.

Fu, Y. X., Shen, Y., Gao, H., & Dan, Y. (2004). Asymmetry in visual cortical circuits underlying motion-induced perceptual mislocalization. *Journal of Neuroscience, 24,* 2165–2171.

Gallant, J. L., Braun, J., & Van Essen, D. C. (1993). Selectivity for polar, hyperbolic, and Cartesian gratings in macaque visual cortex. *Science, 259,* 100–103.

Geisler, W. S. (1999). Motion streaks provide a spatial code formation direction. *Nature, 400,* 65–69.

Geisler, W. S., Albrecht, D. G., Crane, A. M., & Stern, L. (2001). Motion direction signals in the primary visual cortex of cat and monkey. *Visual Neuroscience, 18,* 501–516.

Graziano, M. S. A., Andersen, R. A., & Snowden, R. J. (1994). Tuning of MST neurons to spiral stimuli. *Journal of Neuroscience, 14,* 54–67.

Hedges, J. H., Gartshteyn, Y., Kohn, A., Rust, N. C., Shadlen, M. N., Newsome, W. T., et al. (2011). Dissociation of neuronal and psychophysical responses to local and global motion. *Current Biology, 21,* 2023–2028.

Heeger, D. J. (1992). Normalization of cell responses in cat striate cortex. *Visual Neuroscience, 9,* 181–197.

Heeger, D. J., Simoncelli, E. P., & Movshon, J. A. (1996). Computational models of cortical visual processing. *Proceedings of the National Academy of Sciences, USA, 93,* 623–627.

Holliday, I. E., & Meese, T. S. (2008). Optic flow in human vision: MEG reveals a foveo-fugal bias in V1, specialization for spiral-space in hMSTs, and global motion sensitivity in the IPS. *Journal of Vision*, *8*(10):17, 1–24, http://www.journalofvision.org/content/8/10/17, doi:10.1167/8.10.17. [PubMed] [Article]

Horn, B. K. P., & Brooks, M. J. (Eds.). (1989). *Shape from shading*. Boston: MIT Press.

Jancke, D. (2000). Orientation formed by a spot's trajectory: A two-dimensional population approach in primary visual cortex. *Journal of Neuroscience, 20,* 1–6.

Krekelberg, B., Dannenberg, S., Hoffmann, K. P., Bremmer, F., & Ross, J. (2003). Neural correlates of implied motion. *Nature, 424,* 674–677.

Lagae, L., Maes, H., Raiguel, S., Xiao, D. K., & Orban, G. A. (1994). Responses of macaque STS neurons to optic flow components: a comparison of areas MT and MST. *Journal of Neurophysiology, 71,* 1597–1626.

Lagae, L., Raiguel, S., & Orban, G. A. (1993). Speed and direction selectivity of macaque middle temporal neurons. *Journal of Neurophysiology, 69,* 19–39.

Martin, P., & Hudspeth, A. J. (2001). Compressive nonlinearity in the hair bundle's active response to mechanical stimulation. *Proceedings of the National Academy of Sciences, USA, 98,* 14386–14391.

Mather, G. (1980). The movement after-effect and a distribution shift model of direction coding. *Perception, 9,* 379–392.

Mather, G., Pavan, A., Bellacosa, R. M., & Casco, C. (2012). Psychophysical evidence for interactions between visual motion and form processing at the level of motion integrating receptive fields. *Neuropsychologia, 50,* 153–159.

Maunsell, J. H., & Van Essen, D. C. (1983). Functional properties of neurons in middle temporal visual area of the macaque monkey. I. Selectivity for stimulus direction, speed, and orientation. *Journal of Neurophysiology, 49,* 1127–1147.

McGraw, P. V., Walsh, V., & Barrett, B. T. (2004). Motion-sensitive neurons in V5/MT modulate perceived spatial position. *Current Biology, 14,* 1090–1093.

McGraw, P. V., Whitaker, D., Skillen, J., & Chung, S. T. (2002). Motion adaptation distorts perceived visual position. *Current Biology, 12,* 2042–2047.

Mineault, P. J., Khawaja, F. A., Butts, D. A., & Pack, C. C. (2012). Hierarchical processing of complex motion along the primate dorsal visual pathway. *Proceedings of the National Academy of Sciences, USA, 109,* E972–E980.

Mishkin, M., Ungerleider, L. G., & Macko, K. A. (1983). Object vision and spatial vision: Two cortical pathways. *Trends in Neuroscience, 6,* 414–417.

Morrone, M. C., Burr, D. C., & Vaina, L. M. (1995). Two stages of visual processing for radial and circular motion. *Nature, 376,* 507–509.

Morrone, M. C., Tosetti, M., Montanaro, D., Fiorentini, A., Cioni, G., & Burr, D. C. (2000). A cortical area that responds specifically to optic flow, revealed by fMRI. *Nature Neuroscience, 3,* 1322–1328.

Niehorster, D. C., Cheng, J. C., & Li, L. (2010). Optimal combination of form and motion cues in human heading perception. *Journal of Vision*, *10*(11):20, 1–15, http://www.journalofvision.org/content/10/11/20, doi:10.1167/10.11.20. [PubMed] [Article]

Orban, G., Lagae, L., Verri, A., Raigual, S., Xiao, D., Maes, H., et al. (1992). First order analysis of optical flow in the monkey brain. *Proceedings of the National Academy of Sciences, USA, 89,* 2595–2599.

Ostwald, D., Lam, J. M., Li, S., & Kourtzi, Z. (2008). Neural coding of global form in the human visual cortex. *Journal of Neurophysiology, 99,* 2456–2469.

Pack, C. C., & Born, R. T. (2001). Temporal dynamics of a neural solution to the aperture problem in visual area MT of macaque brain. *Nature, 409,* 1040–1042.

Pack, C. C., Livingstone, M. S., Duffy, K. R., & Born, R. T. (2003). End-stopping and the aperture problem. *Neuron, 39,* 671–680.

Pavan, A., & Mather, G. (2008). Distinct position assignment mechanisms revealed by cross-order motion. *Vision Research, 48,* 2260–2268.

Pelli, D. G. (1997). The VideoToolbox software for visual psychophysics: Transforming numbers into movies. *Spatial Vision, 10,* 437–442.

Price, N. S. C., Greenwood, J. A., & Ibbotson, M. R. (2004). Tuning properties of radial phantom motion aftereffects. *Vision Research, 44,* 1971–1979.

Paninski, L. (2004). Maximum likelihood estimation of cascade point-process neural encoding models. *Network, 15,* 243–262.

Purushothaman, G., Ögmen, H., Chen, S., & Bedell, H. E. (1998). Motion deblurring in a neural network model of retino-cortical dynamics. *Vision Research, 38,* 1827–1842.

Reinhardt-Rutland, A. H. (1994). Perception of motion in depth from luminous rotating spirals: Directional asymmetries during and after rotation. *Perception, 23,* 763–769.

Regan, D., & Beverly, K. I. (1985). Visual responses to vorticity and the neural analysis of optic flow. *Journal of the Optical Society of America A, 2,* 280–283.

Ross, J. (2004). The perceived direction and speed of global motion in glass pattern sequences. *Vision Research, 44,* 441–448.

Rust, N. C., Mante, V., Simoncelli, E. P., & Movshon, J. A. (2006). How MT cells analyze the motion of visual patterns. *Nature Neuroscience, 9,* 1421–1431.

Saito, H.-A., Yukie, M., Tanaka, K., Hikosaka, K., Fukada, Y., & Iwai, E. (1986). Integration of direction signals of image motion in the superior temporal sulcus of the macaque monkey. *Journal of Neuroscience, 6,* 145–157.

Sakata, H., Shibutani, H., Ito, Y., & Tsurugai, K. (1986). Parietal cortical neurons responding to rotary movement of visual stimulus in space. *Experimental Brain Research, 61,* 658–663.

Sakata, H., Shibutani, H., Kawano, K., & Harrington, T. L. (1985). Neural mechanisms of space vision in the parietal association cortex of the monkey. *Vision Research, 25,* 453–463.

Scott, T. R., Lavender, A. D., McWhirt, R. A., & Powell, D. A. (1966). Directional asymmetry of motion after-effect. *Journal of Experimental Psychology, 71,* 806–815.

Simoncelli, E. P., & Heeger, D. J. (1998). A model of neuronal responses in visual area MT. *Vision Research, 38,* 743–761.

Snowden, R. J., & Milne, A. B. (1996). The effects of adapting to complex motions: position invariance and tuning to spiral motions. *Journal of Cognitive Neuroscience, 8,* 435–452.

Snowden, R. J., & Milne, A. B. (1997). Phantom motion after effects: Evidence of detectors for the analysis of optic flow. *Current Biology, 7,* 717–722.

Tadin, D., Lappin, J. S., Gilroy, L. A., & Blake, R. (2003). Perceptual consequences of centre-surround

antagonism in visual motion processing. *Nature, 424,* 312–315.

Tanaka, K., Fukada, Y., & Saito, H. (1989). Underlying mechanisms of the response specificity of the expansion/contraction and rotation cells in the dorsal part of the medial superior temporal area of the macaque monkey. *Journal of Neurophysiology, 62,* 642–656.

Tanaka, K., Hirosaka, K., Saito, H., Yukie, M., Fukuda, Y., & Iwai, E. (1986). Analysis of local and wide-field movements in the superior temporal visual areas of the macaque monkey. *Journal of Neuroscience, 6,* 134–144.

Tanaka, K., & Saito, H. (1989). Analysis of motion of the visual field by direction, expansion/contraction, and rotation cells clustered in the dorsal part of the medial superior temporal area of the macaque monkey. *Journal of Neurophysiology, 62,* 626–641.

Tanaka, K., Sugita, Y., Moriya, M., & Saito, H. (1993). Analysis of object motion in the ventral part of the medial superior temporal area of the macaque visual cortex. *Journal of Neurophysiology, 69,* 128–142.

Takemura, A., Murata, Y., Kawano, K., & Miles, F. A. (2007). Deficits in short-latency tracking eye movements after chemical lesions in monkey cortical areas MT and MST. *Journal of Neuroscience, 27,* 529–541.

Tootell, R. B., & Hadjikhani, N. (2001). Where is "dorsal V4" in human visual cortex? Retinotopic, topographic and functional evidence. *Cerebral Cortex, 11,* 298–311.

Ungerleider, L. G., & Desimone, R. (1986). Cortical connections of visual area MT in the macaque. *Journal of Comparative Neurology, 248,* 190–222.

van der Smagt, M. J., Verstraten, F. A., & van de Grind, W. A. (1999). A new transparent motion aftereffect. *Nature Neuroscience, 2,* 595–596.

Verstraten, F. A., Fredericksen, R. E., & van de Grind, W. A. (1994). Movement aftereffect of bi-vectorial transparent motion. *Vision Research, 34,* 349–358.

Verstraten, F. A., van der Smagt, M. J., Fredericksen, R., & van de Grind, E. W. A. (1999). Integration after adaptation to transparent motion: Static and dynamic test patterns result in different aftereffect directions. *Vision Research, 39,* 803–810.

von Grünau, M. W. (2002). Bivectorial transparent stimuli simultaneously adapt mechanisms at different levels of the motion pathway. *Vision Research, 42,* 577–587.

Weisstein, N., Maguire, W., & Berbaum, K. (1977). A phantom-motion aftereffect. *Science, 198,* 955–958.

Whitney, D. (2002). The influence of visual motion on perceived position. *Trends in Cognitive Science, 6,* 211–216.

Wu, M. C. K., David, S. V., & Gallant, J. L. (2006). Complete functional characterization of sensory neurons by system identification. *Annual Review of Neuroscience, 29,* 477–505.